Available online at www.sciencedirect.com
SCIENCE DIRECT®
Journal of Chromatography A, 1010 (2003) 153–176
JOURNAL OF CHROMATOGRAPHY A
www.elsevier.com/locate/chroma

Adsorption–desorption isotherm hysteresis of phenol on a C_{18}-bonded surface

Fabrice Gritti[a,b], Georges Guiochon[a,b,*]

[a]*Department of Chemistry, University of Tennessee, Knoxville, TN 37996-1600, USA*
[b]*Division of Chemical Sciences, Oak Ridge National Laboratory, Oak Ridge, TN 37831-6120, USA*

Received 3 April 2003; received in revised form 4 June 2003; accepted 10 June 2003

Abstract

Single component adsorption and desorption isotherms of phenol were measured on a high-efficiency Kromasil-C_{18} column (N=15 000 theoretical plates) with pure water as the mobile phase. Adsorption isotherm data were acquired by frontal analysis (FA) for seven plateau concentrations distributed over the whole accessible range of phenol concentration in pure water (5, 10, 15, 20, 25, 40, and 60 g/l). Desorption isotherm data were derived from the corresponding rear boundaries, using frontal analysis by characteristic points (FACP). A strong adsorption hysteresis was observed. The adsorption of phenol is apparently modeled by a S-shaped isotherm of the first kind while the desorption isotherm is described by a convex upward isotherm. The adsorption breakthrough curves could not be modeled correctly using the adsorption isotherm because of a strong dependence of the accessible free column volume on the phenol concentration in the mobile phase. It seems that retention in water depends on the extent to which the surface is wetted by the mobile phase, extent which is a function of the phenol concentration, and of the local pressure rate, which varies along the column, and on the initial state of the column. By contrast, the desorption profiles agree well with those calculated with the desorption isotherms using the ideal model, due to the high column efficiency. The isotherm model accounting best for the desorption isotherm data and the desorption profiles is the bi-Langmuir model. Its coefficients were calculated using appropriate weights in the fitting procedure. The evolution of the bi-Langmuir isotherm parameters with the initial equilibrium plateau concentration of phenol is discussed. The FACP results reported here are fully consistent with the adsorption data of phenol previously reported and measured by FA with various aqueous solutions of methanol as the mobile phase. They provide a general, empirical adsorption model of phenol that is valid between 0 and 65% of methanol in water.
© 2003 Elsevier B.V. All rights reserved.

Keywords: Adsorption isotherms; Adsorption–desorption hysteresis; Frontal analysis; Band profiles; Mobile phase composition; Mathematical modeling; Phenols

1. Introduction

The retention of analytes in chromatography depends on their distribution between the stationary and the mobile phases, considered as two immiscible phases in direct contact, allowing fast transfer of the solute from one phase to the other. It is assumed, most often implicitly, that the adsorption properties of the adsorbent remain constant when the analyte partial pressure or its concentration increases from

*Corresponding author. Tel.: +1-865-974-0733; fax: +1-865-974-2667.
E-mail address: guiochon@utk.edu (G. Guiochon).

0021-9673/03/$ – see front matter © 2003 Elsevier B.V. All rights reserved.
doi:10.1016/S0021-9673(03)01071-9

zero to the highest value possible, i.e. its vapor pressure or its solubility in gas or liquid chromatography, respectively. As long as this assumption is fulfilled, theoretical adsorption models may be applied to describe the behavior of the experimental adsorption data. This is true as long as the mobile phase does not perturb the surface of the solid adsorbent (e.g. in gas–solid equilibria [1]). In liquid–solid equilibria, Guiochon et al. [2] have reviewed a large number of extended gas–solid isotherms which were used successfully to describe eclectic experimental situations. However, difficulties are encountered in RPLC in which the C_{18}-bonded silica surface exhibit properties that are often considered to belong to a liquid–liquid interface. The nature of the mobile phase influences the structure of the layer of the bonded alkyl chains, hence the sorption properties of the surface. For example, the use of organic solvents (e.g. acetonitrile (ACN), MeOH, tetrahydrofuran (THF)) [3–8] and, to a larger extent, that of ionic or non-ionic surfactants [9–13] as aqueous mobile phase modifiers affects the properties of the adsorbent surface due to their compelling adsorption. Accordingly, as soon as a solute is injected, the adsorbent properties are somewhat modified, which perturbs the solute adsorption itself. This effect is particularly important at high concentrations, as used in preparative liquid chromatography. The structure and the surface energy distribution of the stationary phase and the adsorption of the solute are related phenomena which are controlled by the equilibrium of formation of the interfacial phase. In most cases, this equilibrium is achieved very rapidly. Then, adsorption can be considered alone. When this equilibrium is reached more slowly than adsorption itself, these two phenomena cannot be considered separately. Otherwise, serious difficulties arise in the accurate modeling of band profiles at high concentrations or in gradient elution chromatography with strongly adsorbed solvent modifiers. A correct modeling of chromatography would then require the knowledge of the relevant kinetic data, the rate of equilibration of the interfacial region when the solute and/or the solvent modifier concentration in the mobile phase change during the chromatographic process.

In an earlier work, we measured the adsorption–desorption equilibrium data of phenol on a C_{18}-bonded silica column using aqueous solutions of methanol as the mobile phase [14]. The equilibrium was found to be reversible and well modeled by a bi-Langmuir isotherm. This made possible a study of the dependence of the saturation capacity on the mobile phase composition. When organic modifiers other than methanol (e.g. ACN, isopropanol, THF) were used for a similar study, unexpected band profiles were obtained for phenol. The shape of these profiles suggested that they should be considered as the results of a binary competition between phenol and the organic modifier rather than arising from the non-linear adsorption of single components from an inert solvent [15]. It became necessary to determine the adsorption isotherm of phenol from water on the Kromasil-C_{18} column used. In this determination, we have to revisit the difficult situation, known for a long time in RPLC, of the elution on a C_{18}-bonded silica by water which does not wet this packing material. Water does not wet the surface of RPLC packing materials. When particles of such a material are spread over water, they float while they sink in methanol. Accordingly, the contact angle of water on a silanized surface is larger than 90° and pure water can penetrate the pores only under pressure and to an extent limited by the Washburn equation [16], which relates the radius of a pore opening and the pressure needed to fill it with a liquid that does not wet the walls of the pore (see later, Section 2, Eq. (1)). Assuming the same wetting angle for water as for mercury (130°), we can estimate that pores larger than 0.100 and 0.010 μm (i.e. 1000 and 100 Å) are filled under pressures of 1 and 10 MPa (i.e. 10 and 100 bar), respectively. Because 20% of the total pore volume of Kromasil only are larger than 100 Å [16], we can expect that Kromasil is not soaked by pure water, which it is easy to verify by spreading a little amount of it over water.

Thus, chromatographic results depend on the initial state of the column. If the column is filled with pure water, the pores are not wet and retention is small. If the column is filled with an aqueous solution of methanol and the methanol concentration is ramped down, part of the pores remain filled since water does not empty the pores immediately. Retention depends on the amount of water remaining in the pores, which probably depends on the local pressure (decreasing linearly from the column inlet

to its outlet), hence on the flow rate, and on the equilibration rate of the stationary phase upon a change in the composition of the mobile phase percolating the column. The situation is further complicated when measurements are made at high concentrations of an organic solvent. The surface tension of the aqueous solution decreases rapidly with increasing organic content and the contact angle increases. The extent of water penetrating inside the pores of the particles increases and so should retention do.

A detailed investigation of this situation is the goal of this work. Phenol was selected as the solute and will be used as the organic modifier as well because it is easy to detect and because its adsorption was previously studied on the same column [14]. In this work, the adsorption isotherms were measured by FA and the desorption isotherms by FACP, using the same concentration plateaus. The adsorption–desorption isotherms exhibit clear hysteresis loops. Pressure has a considerable influence on the results, as expected.

2. Theory

2.1. The Washburn equation

As aforementioned in Section 1, the Wasburn equation relates the radius of the pore opening and the pressure that must be applied to a liquid to fill them. This equation is:

$$P = \frac{-2\gamma}{r_p}\cos(\theta) \quad (1)$$

where γ is the surface tension between the liquid and the surface of the adsorbent studied, r_p is the radius of the pores and θ is the advancing contact angle between the liquid and the adsorbent surface.

2.2. Determination of the adsorption isotherm by frontal analysis (FA)

Frontal analysis (FA) was used to determine the single-component adsorption isotherm data of phenol [2,17,18]. It consists in the replacement of the stream of the mobile phase percolating through the column with a stream of a solution of the studied compound. The breakthrough curve is recorded. Then, the column is washed with the pure mobile phase and the same experiment is repeated with a more concentrated solution. Mass conservation of the solute between the times when the new solution enters the column and when the plateau concentration is reached allows the calculation of the mass, m_t^*, of solute retained in the column at equilibrium with a given mobile phase concentration, C. This mass is best measured by integrating the breakthrough curve (equal area method) [19]. The amount m_t^* is given by:

$$m_t^* = CV_{eq} \quad (2)$$

where V_{eq} is the elution volume of the equivalent area of the solute. Note that m_t^* is not the mass adsorbed but the total mass present in the whole column either adsorbed or in solution in the void volume. The knowledge of this latter volume (i.e. the volume actually occupied by the solution of concentration C in the column) allows the determination of the adsorbed amount q_a^* per unit of adsorbent volume by:

$$q_a^* = \frac{m_t^* - CV_0}{V_a} \quad (3)$$

where V_0 and V_a are the column void volume and the adsorbent volume, respectively.

2.3. Determination of the desorption isotherm by frontal analysis by characteristic points (FACP)

In the case or reversible adsorption–desorption processes, the measurement of the single-component adsorption isotherm can be performed also from the rear boundary recorded in FA when replacing the solution with the pure mobile phase so long as the column efficiency is high enough [20]. This is the FACP method [21]. In principle, this method gives the desorption isotherm. The mass balance written for each point of the rear boundary of the profile allows the calculation of the amount adsorbed by integration of this boundary, starting from the tail end ($C=0$) [2]. The desorbed amount q_d^* of solute from $C=0$ to $C=C^*$ per unit of adsorbent volume is:

$$q_d^* = \frac{1}{V_a}\int_0^{C^*} (V - V_0)\, dC \quad (4)$$

where V is the retention volume of the point of the rear diffuse boundary at concentration C, called a characteristic point.

2.4. Models of isotherm

Three isotherm models were used, all based on the Langmuir model to describe the desorption isotherm of phenol, the Langmuir, the bi-Langmuir, and a further extension, the tri-Langmuir isotherm models.

2.4.1. The Langmuir isotherm

This model is the most frequently used in general studies of liquid–solid chromatographic equilibria, in spite of its semi-empirical nature [22,23]. It is written:

$$q^* = q_s \frac{bC}{1 + bC} \quad (5)$$

In this model, q_s is the monolayer saturation capacity of the adsorbent and b is the equilibrium constant of adsorption. This model assumes that the surface of the adsorbent is homogeneous, that adsorption is localized, and that there are no adsorbate–adsorbate interactions. The equilibrium constant b is given by the following equation [24]:

$$b = b_0\, e^{\epsilon_a/RT} \quad (6)$$

where ϵ_a is the energy of adsorption, R is the universal ideal gas constant, T is the absolute temperature and b_0 is a preexponential factor that could be derived from the molecular partition functions in both the bulk and the adsorbed phases. Consistent with the basic assumption of this model, the adsorption energy distribution (AED) function, $F(\epsilon)$, of the Langmuir isotherm is a Dirac function:

$$F(\epsilon) = q_s \delta(\epsilon - \epsilon_a) \quad (7)$$

The AED function characterizes the heterogeneity of the surface. A surface on which a compound adsorbs following Langmuir isotherm behavior is homogeneous for this compound. Then, the AED is unimodal, with a mode width equal to 0.

2.4.2. The bi-Langmuir and the tri-Langmuir isotherms

The bi-Langmuir model is the simplest model for a non-homogeneous surface [25]. It can easily be extended to a tri-Langmuir model. The surface is assumed to be paved with two or three different types of homogeneous chemical domains which behave independently. Then, the equilibrium isotherm results from the addition of two or three independent local Langmuir isotherms:

$$q^* = q_{s,1}\frac{b_1 C}{1 + b_1 C} + q_{s,2}\frac{b_2 C}{1 + b_2 C} \quad (8)$$

for the bi-Langmuir isotherm and

$$q^* = q_{s,1}\frac{b_1 C}{1 + b_1 C} + q_{s,2}\frac{b_2 C}{1 + b_2 C} + q_{s,3}\frac{b_3 C}{1 + b_3 C} \quad (9)$$

for the tri-Langmuir isotherm.

In these models, there are one, two, or three saturation capacities, $q_{s,1}$, $q_{s,2}$ and $q_{s,3}$, that are related to the surface area of each one of the different types of sites existing on the surface. The equilibrium constants b_1, b_2, and b_3 are associated with the adsorption energies $\epsilon_{a,1}$, $\epsilon_{a,2}$, and $\epsilon_{a,3}$, through Eq. (6). The AED functions become:

$$F(\epsilon) = q_{s,1}\delta(\epsilon - \epsilon_{a,1}) + q_{s,2}\delta(\epsilon - \epsilon_{a,2}) \quad (10)$$

or

$$F(\epsilon) = q_{s,1}\delta(\epsilon - \epsilon_{a,1}) + q_{s,2}\delta(\epsilon - \epsilon_{a,2}) + q_{s,3}\delta(\epsilon - \epsilon_{a,3}) \quad (11)$$

These energy distributions are bimodal or trimodal and all their modes have a width 0.

2.5. Calculation of the adsorption energy distributions

Actual surfaces are neither homogeneous nor paved with homogeneous tiles, as was assumed so far. These surfaces are characterized by an AED having a finite width. The experimental isotherm on such a surface is the sum of the isotherms on each one of the homogeneous fractions of the surface, fractions that correspond to given energies of the AED. Under the condition of a continuous distribu-

tion and assuming a Langmuir local isotherm model, this sum can be replaced by an integral and the overall adsorption isotherm can be written [24]:

$$q^*(C) = \int_0^\infty F(\epsilon)\frac{b(\epsilon)C}{1+b(\epsilon)C}\,d\epsilon \quad (12)$$

where $q^*(C)$ is the total amount of solute adsorbed on the surface at equilibrium with a concentration C, ϵ is the binding energy between an adsorbed solute molecule and the surface of the adsorbent, b is the associated binding constant and is related to ϵ though Eq. (6).

The normalization condition for the AED is

$$\int_0^\infty F(\epsilon)d\epsilon = q_s \quad (13)$$

where q_s is the overall saturation capacity.

To characterize the behavior of a heterogeneous surface, the AED, $F(\epsilon)$, is derived from the isotherm data (M data points), a procedure for which there is a variety of methods [24,26–28]. Most of these methods use a preliminary smoothing of the experimental data, fitting the smoothed data to an isotherm model, or search for an AED given by a certain function. In both cases, arbitrary information is injected in the determination of the AED. In this work, the EM method [28] was used. This computer-intensive method uses directly the raw experimental data, without injecting any arbitrary information into the derivation. The distribution function $F(\epsilon)$ is discretized using an N-grid points in the energy space (i.e. assuming that the surface is made of a set of N homogeneous surfaces) and the corresponding values of $F(\epsilon)$ are estimated from the data points. The energy space is limited by ϵ_{min} and ϵ_{max}. These energy boundaries are obtained from the maximum and minimum concentrations within which the adsorption data have been acquired, by using Eq. (6) (with $b_{min}=1/C_{max}$, $b_{max}=1/C_{min}$) but a narrower range may be considered as long as it accommodates the data. The amount $q(C_j)$ of solute adsorbed at concentration C_j is iteratively estimated by:

$$q^k_{cal}(C_j) = \sum_{\epsilon_{min}}^{\epsilon_{max}} F^k(\epsilon_i)\frac{b(\epsilon_i)C_j}{1+b(\epsilon_i)C_j}\Delta\epsilon$$
$$j\in[1,M];\ i\in[1,N] \quad (14)$$

with

$$\Delta\epsilon = \frac{\epsilon_{max}-\epsilon_{min}}{N-1} \qquad \epsilon_i = \epsilon_{min} + (i-1)\Delta\epsilon \quad (15)$$

The index k indicates the kth iteration of the numerical calculation of the AED function. The initial guess (iteration $k=0$) of the AED function $F(\epsilon_i)$ is the uniform distribution (over the N fictitious adsorption sites) of the maximum adsorbed amount observed experimentally. This initial guess has the advantage of introducing the minimum bias into the AED calculation.

$$F^0(\epsilon_i) = \frac{q(C_M)}{N} \quad \forall i\in[1,N] \quad (16)$$

Actually, the EM program calculates the amount adsorbed by taking $b(\epsilon_i)$ as the variable in the energy space, so that neither the temperature nor the pre-exponential factor need to be defined. Only M, N, b_{min}, b_{max} and the number of iterations must be defined before starting the calculations. b_{min} and b_{max} are related to the reciprocal of the highest and the lowest concentrations applied in FA, respectively. It is noteworthy that, to obtain any information on the adsorption energy, an assumption must be made for b_0 in Eq. (6). The final result is the distribution of the equilibrium constants.

The distribution function is updated after each iteration by:

$$F^{k+1}(\epsilon_i) = F^k(\epsilon_i)\sum_{C_{min}}^{C_{max}}\frac{b(\epsilon_i)C_j}{1+b(\epsilon_i)C_j}\Delta\epsilon\,\frac{q_{exp}(C_j)}{q^k_{cal}(C_j)} \quad (17)$$

The EM procedure protects better than most other methods against the consequences of the possible incorporation of experimental artifacts into the calculation of the AED or against the effect of modeling the experimental data (and particularly the noise and drift that the data may contain).

2.6. Modeling of desorption-band profiles in HPLC

The desorption band profiles from the different equilibrium plateau concentrations were calculated, using the desorption isotherm derived from the data acquired by FACP and the equilibrium-dispersive (ED) model of chromatography [1,2,29]. The raw experimental data were also used directly for a similar calculation (or rather the 3000 data points

derived from the diffuse boundaries recorded; interpolation between these points was done, assuming a non-physical Taylor development of the third order between two consecutive experimental data points). This procedure alleviates, to some extent, the circular argument of using ECP or FACP, i.e. chromatographic methods, to derive an isotherm and then using this isotherm to calculate the profiles of chromatographic signals. The ED model assumes instantaneous equilibrium between mobile and stationary phases and a finite column efficiency originating from an apparent axial dispersion coefficient, D_a, that accounts for the dispersive phenomena (molecular and eddy diffusion) and for the non-equilibrium effects that take place in a chromatographic column. The axial dispersion coefficient is:

$$D_a = \frac{uL}{2N} \tag{18}$$

where u is the mobile phase linear velocity, L the column length, and N is the number of theoretical plates or apparent efficiency of the column, measured under linear conditions, i.e. with a small sample size.

In this model, the mass balance equation for a single component is written:

$$\frac{\partial C}{\partial t} + u\frac{\partial C}{\partial z} + F\frac{\partial q^*}{\partial t} - D_a\frac{\partial^2 C}{\partial z^2} = 0 \tag{19}$$

where q^* and C are the stationary and mobile phase concentrations of the adsorbate, respectively, t is the time, z the distance along the column, and $F=(1-\epsilon_t)\epsilon_t$ is the phase ratio, with ϵ_t the total column porosity. q^* is related to C through the isotherm equation, $q^*=f(C)$.

2.6.1. Initial and boundary conditions for the ED model

At $t=0$, the concentrations of the solute and the adsorbate in the column are uniformly equal to zero, and the stationary phase is in equilibrium with the pure mobile phase. The boundary conditions used are the classical Danckwerts-type boundary conditions [2,30] at the inlet and outlet of the column.

2.6.2. Numerical solutions of the ED model

The ED model was solved using a computer program based on an implementation of the method of orthogonal collocation on finite elements (OCFE) [31–33]. The set of discretized ordinary differential equations was solved with the Adams–Moulton method, implemented in the VODE procedure [34]. The relative and absolute errors of the numerical calculations were 10^{-6} and 10^{-8}, respectively.

3. Experimental

3.1. Chemicals

The mobile phase used in this work was HPLC grade water, purchased from Fisher Scientific (Fair Lawn, NJ, USA). The solvents used to prepare the mobile phase were filtered before use on an SFCA filter membrane, 0.2 μm pore size (Suwannee, GA, USA). ACN, purchased from the same company, was used as the mobile phase to determine the maximum column void volume. Thiourea was chosen to measure the column hold-up volume. Phenol was used as the solute in this study. Both thiourea and phenol were obtained from Aldrich (Milwaukee, WI, USA).

3.2. Materials

A manufacturer-packed, 250×4.6 mm Kromasil column was used (Column E6021, Eka Nobel, Bohus, Sweden). This column was packed with a C_{18}-bonded, endcapped, porous silica. It was one of the lot of ten columns (Columns E6019, E6103–E6106, E6021–E6024 and E6436) previously used by Kele [35] and Gritti [36] for their studies of the reproducibility of the chromatographic properties of RPLC columns under linear [35] and non-linear [36] conditions, respectively. The main characteristics of the bare porous silica and of the packing material used are summarized in Table 1.

The hold-up time of this column was derived from the retention time of thiourea injections. Uracil is not satisfactory for this purpose because it is retained when pure water is used as the mobile phase (the retention factor is ca. 1).

3.3. Apparatus

The isotherm data were acquired using a Hewlett–Packard (Palo Alto, CA, USA) HP 1090 liquid chromatograph. This instrument includes a multi-solvent delivery system (tank volumes, 1 l each), an

Table 1
Physico-chemical properties of the packed Kromasil-C_{18} (Eka) #E6021 column

Particle size (μm)	5.98
Particle size distribution (90:10, percentage ratio)	1.44
Pore size (Å)	112
Pore volume (ml/g)	0.88
Surface area (m^2/g)	314
Na, Al, Fe content (ppm)	11; <10; <10
Particle shape	Spherical
Total carbon (%)	20.0
Surface coverage (μmol/m^2)	3.59
Endcapping	Yes

auto-sampler with a 250 μl sample loop, a diode-array UV-detector, a column thermostat and a data station. Compressed nitrogen and helium bottles (National Welders, Charlotte, NC, USA) are connected to the instrument to allow the continuous operations of the pump, the auto-sampler, and the solvent sparging. The extra-column volumes are 0.068 and 0.90 ml as measured from the auto-sampler and from the pump system, respectively, to the column inlet. All the retention data were corrected for this contribution. The flow-rate accuracy was controlled by pumping the pure mobile phase at 23 °C and 1 ml/min during 50 min, from each pump head, successively, into a volumetric glass of 50 ml. The relative error was less than 0.4%, so that we can estimate the long-term accuracy of the flow-rate at 4 μl/min at flow rates around 1 ml/min. All measurements were carried out at a constant temperature of 23 °C, fixed by the laboratory air-conditioner. The daily variation of the ambient temperature never exceeded ±1 °C.

3.4. Measurements of the adsorption isotherms by FA and of the desorption isotherms by FACP

The solubility of phenol in water is approximately 67 g/l. The desorption of phenol was so slow at high concentrations that it was impossible to carry out a large number of consecutive FA runs. Only seven phenol concentrations were then applied for the determination of the adsorption isotherm: 5, 10, 15, 20, 25, 40, and 60 g/l. One pump of the HPLC instrument was used to deliver a stream of the pure mobile phase (water), the second pump a stream of the pure sample solution, an aqueous solution of phenol at 60 g/l. The concentration of phenol in the FA stream is determined by the concentration of the mother sample solution and the flow-rate fractions delivered by the two pumps. The breakthrough curves were recorded at a flow rate of 1 ml/min, with a sufficiently long time delay between each breakthrough curve to allow for the reequilibration of the column with the pure mobile phase. The injection time of the sample was fixed at 45 min for all FA steps in order to reach a stable plateau at the column outlet. To avoid recording any UV-absorbance signal larger than 1500 mAU and the corresponding signal noise, the detector signal was detected at 291 nm for all mobile phases. The detector response for phenol was calibrated accordingly. For reasons explained later, in order to begin each new experiment from a well-defined, reproducible initial state, the flow rate is dropped to zero after the end of the acquisition of each new desorption rear profile, in order to let the pressure inside the column and inside the pores of the particles become equal to the atmospheric pressure. The acquisition of the adsorption data points at 20 g/l was repeated twice, but without cutting off the flow rate between the two runs, to compare the results of the two procedures. These measurements were performed at different flow rates to investigate the influence of the pressure on the results. The pressure inside the column was increased by connecting a length of approximately 30 cm of an approximately 0.0625 mm (exactly, 0.0025 in.) I.D. polyether ether ketone (PEEK) tubing downstream the detector. This raised the outlet column pressure to approximately 140 bar at a water flow rate of 1 ml/min.

The desorption isotherm was derived from the profile of the desorption band of phenol obtained by pumping pure water in the column, after the column had been previously equilibrated during 45 min with the given water–phenol mixture (see Section 2.2).

4. Results and discussion

4.1. Wetting of the C_{18}-Kromasil surface by water

ACN and water-poor aqueous solutions of ACN wet completely the surface of C_{18}-Kromasil [37,38]. Yet, the cosine of the advancing contact angle is smaller than 1 for ACN and for its concentrated

aqueous solutions. It decreases with increasing water concentration and becomes negative at some intermediate water concentration beyond which the contact angle is larger than 90°. It is unclear, however, exactly for which water concentration it becomes negative and the solution no longer wets the surface but tends to be expelled from the pores. Yet, it has been established that the equilibrium position of the meniscus in a capillary tube is reached very slowly [38]. Suspensions of particles of C_{18}-silica in ACN-rich aqueous solutions are stable, even under mere atmospheric pressure, and the particles do not float. The wetting of the surface of C_{18}-bonded silica by pure water is certainly energetically unfavorable [38]. When pressure is released after the column has been previously filled with pure water (for instance, by decreasing stepwise the ACN content in the mobile phase maintained under pressure by a constant flow rate of 1 ml/min), water molecules are expelled from the mesopores. The phenomenon is nearly complete in less than approximately 1 h. A series of experiments illustrates this unusual behavior.

Fig. 1 shows the variation of the thiourea retention volume, usually the best estimate of the column hold-up volume, with decreasing ACN concentration, down to a pure water mobile phase. As long as the pump is working, the eluent stream is on, and the pressure remains applied to the column, water percolates through the apolar C_{18} modified surface. The

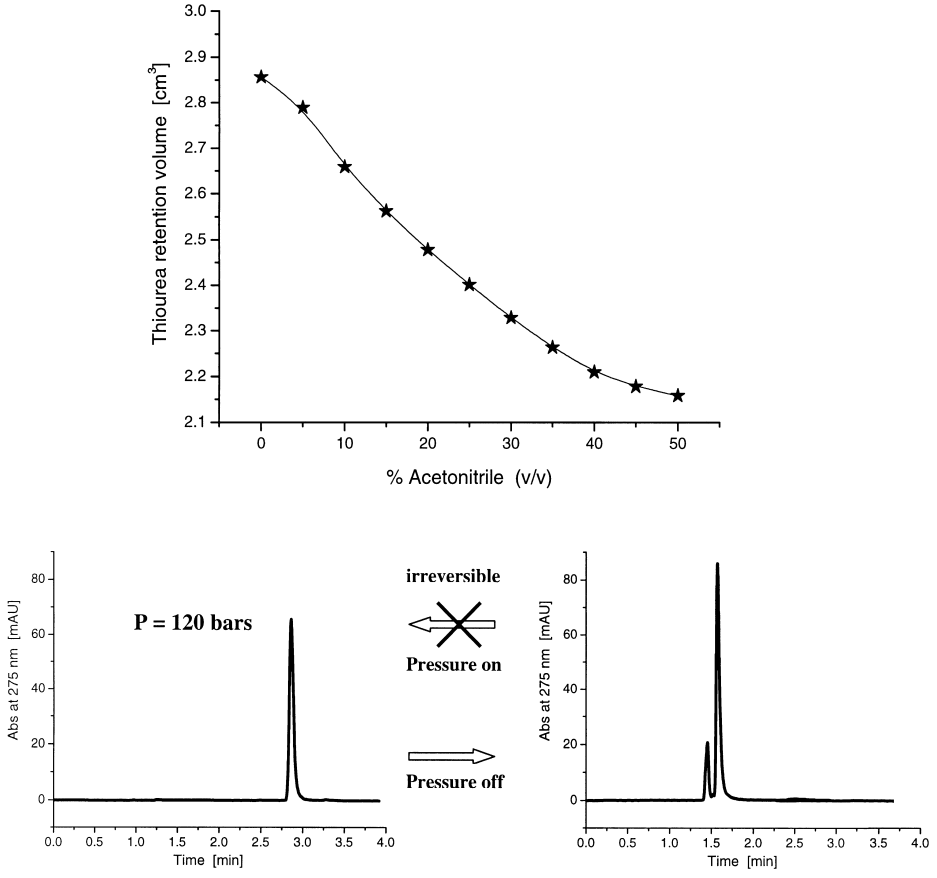

Fig. 1. Effect of the mobile phase composition and the flow rate on the column hold-up volume. Upper graph. Plot of the retention time of thiourea vs. the volume fraction of ACN in the aqueous mobile phase. The ACN fraction was decreased by 5% steps from ACN/water (50:50, v/v) to pure water. Lower left graph. Chromatogram of thiourea recorded at the end of the series of measurements of the hold-up volume (i.e. with pure water). Lower right graph. Chromatogram of thiourea injected an hour later, after the flow rate had been cut off.

hold-up volume increases. This result does not mean that pure water (or ACN-poor aqueous solutions) wets the surface better than ACN-rich aqueous solutions nor that it has access to smaller mesopores. Actually, the hold-up volume increases because the structure of the alkyl chains in the interfacial region collapses. These chains abandon their trans-conformation and fold against the silica surface when ACN is progressively removed. When the proportion of ACN decreases from 50 to 0%, the reduction of the hold-up volume is about 0.7 ml, a considerable change of more than 30% of the initial volume.

However, because the contact angle of water on C_{18}-bonded silica surfaces is larger than 90° [38], the situation of the Kromasil-C_{18} particles impregnated with water is unstable. When the mobile phase flow rate is cut off, water gets irreversibly out of the mesopore structure. When the pressure and the water stream are restored, water penetrates back into the pores only as much as indicated by Washburn equation [16] (see Section 1). Evidence of this phenomenon is illustrated in Fig. 1 by the two elution profiles recorded for the non-retained thiourea, the first one just before the flow rate was cut-off and the second 1 h 30 min later. Before the pressure was released, the retention volume of thiourea was about 2.9 ml, corresponding to the maximum column total porosity of 0.70. After the pressure was released, then restored to its initial value and the mobile phase stream resumed, the volume accessible to thiourea is reduced to 1.6 ml because water cannot reenter the mesopores. It costs too much in terms or surface energy and water molecules have only access to the macropore and part of the mesopore network. The mesopores are then filled with vapors of water and ACN in equilibrium with the liquid phase, and a meniscus forms in the pore opening. The hold-up volume of 1.6 ml corresponds to a total column porosity of 0.38, which is approximately the external porosity of a column packed with spherical particles. For instance, Al-Bokari et al. [39] measured by inverse-size exclusion chromatography the external porosity (0.386) of a column packed with Luna Prep Silica C_{18} of identical size (25×0.46 cm) packed with 10 μm particles instead of 6 μm for our Kromasil column. Note that the peak of thiourea in the chromatogram is preceded by that of another, unidentified compound. The relative height of the two peaks depends strongly on the wavelength at which the column effluent is monitored.

4.2. Adsorption of phenol from pure water onto C_{18}-Kromasil silica

The results shown in the previous section imply that the C_{18}-Kromasil column, once filled with pure water, may exist under one of two different states. The first state corresponds to the macropore space and part of the mesopore network (possibly ca. 20%) only being filled with water molecules. The second state corresponds to the macropore and the mesopore space being both filled with water. For the sake of consistency, we carried out first a series of FA runs starting from the state in which water had no access to the mesopores. In a second experiment, for a plateau concentration of phenol of 20 g/l, we measured and compared the amounts of phenol adsorbed in two different FA runs, starting from each one of the two different possible ‘‘initial states’’ of the column.

The experimental results of the first series are gathered in Fig. 2 which shows the breakthrough curves for six plateau concentrations of phenol applied (second column) and the diffuse rear boundary under logarithmic coordinate (third column). Note that the profiles of the breakthrough curves vary considerably with the phenol concentration (second column). For the lowest concentration (5 g/l, top), a very early, simple shock is observed and rapid column equilibration takes place. The next four plateaus (10, 15, 20 and 25 g/l, the later not shown) exhibit the same initial shock followed by a slow increase of the concentration up to the final plateau. Finally, for the 40 and 60 g/l plateaus, a succession of two or three shocks is recorded, suggesting a faster column equilibration than for the four precedent concentration plateaus. Note that the heights and the retention times of the initial shock layer of each breakthrough curve are nearly the same for all six profiles. By contrast, the second shock takes place earlier in the last case (60 g/l) than at 40 g/l.

The evolution trend of these breakthrough curves suggests that either kinetics effects or the progressive wetting of an increasing fraction of the adsorbent

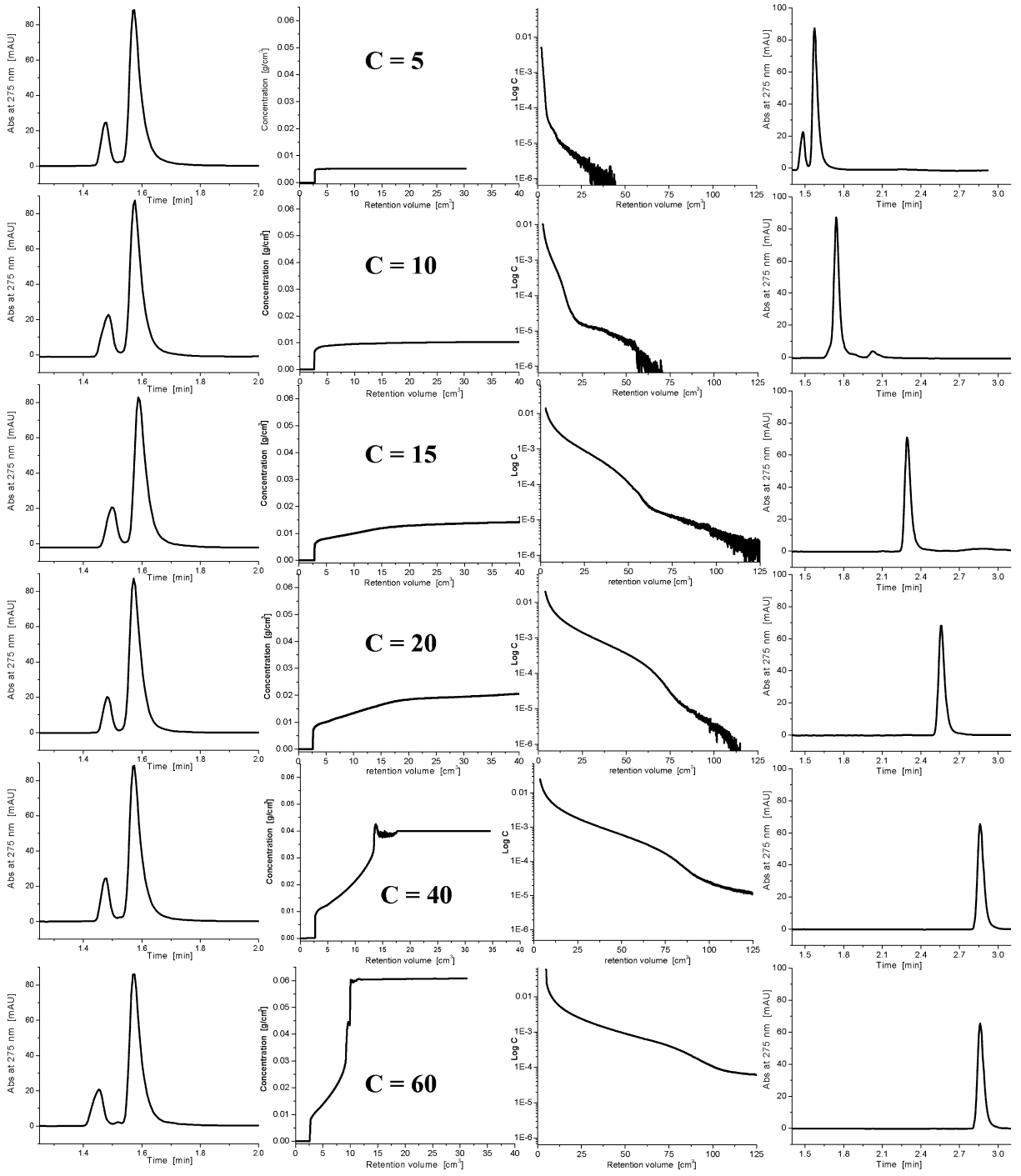

Fig. 2. Results of a series of six FA/FACP experiments at different equilibrium plateau concentrations (5, 10, 15, 20, 25 and 60 g/l of phenol in pure water). $T = 295$ K. Flow rate constant at 1 ml/min. The first column shows the chromatograms of thiourea just before each run. They are all identical, hence water occupies the same volume just before all the adsorption of phenol. The second column shows the six breakthrough curves recorded during adsorption. Note their unusual shape. The third column shows the six desorption profiles (plot of log C vs. time). Note the strong difference in between the retention of phenol, particularly at low concentrations. The fourth column shows the chromatograms of thiourea (same injection as in the first column) just after the complete desorption of phenol. Note that water does not occupy the same volume as before phenol adsorption.

surface by a solution, the surface tension of which decreases with increasing phenol concentration, must be taken into account to explain them. The amount of phenol adsorbed can be measured readily from these curves, using a simple integral mass balance. However, to derive the mass of phenol adsorbed on the C_{18}-bonded silica, the column hold-up volume in presence of the water-phenol solution at equilibrium with the solid interface must be known. Unfortunately, the UV signal of phenol, even at the lowest concentration (5 g/l), is too high and completely prevents the detection of thiourea, whatever the wavelength considered in the whole UV spectrum. Thus, no direct measurements of the hold-up volume of the column at any plateau concentration of phenol were possible. Estimates of this hold-up volume could only be extrapolated to the value measured after phenol was completely removed from the column by pumping pure water. We observed, however, that, while the chromatograms of thiourea recorded just before each breakthrough experiment were identical (Fig. 2, first column), the chromatograms of thiourea recorded just after the end of the diffuse boundaries (when the phenol concentration is 0) were quite different (Fig. 2, last column). In the same way as water does not leave the mesopores in which it has been introduced beforehand with ACN (see later, Section 4.1), so we assumed that, provided the flow rate (hence the pressure gradient along the column) remains constant, the water molecules that have entered the mesopores with phenol stay there when phenol is washed away but that the phenol molecules leaving these pores will not be replaced. The hold-up volumes are derived from the elution times of the thiourea peaks shown in Fig. 2 (last column). These volumes increase with increasing plateau concentration of phenol. Phenol plays the same role as a surfactant (or an organic modifier like ACN), decreases the surface tension of the solution, and increases the fraction of the absorbent surface which is wet. The experimental adsorption data are finally calculated according to these hold-up volumes and the adsorption data and adsorption isotherm of phenol are shown in Fig. 3.

Since only seven isotherm data points were measured, the isotherm cannot be modeled accurately. It is best described by a S-shaped isotherm of the first kind (i.e. it is convex downward at low concentrations, convex upward at high concentrations). By contrast to other systems [40], however, it seems that, in the present case, this isotherm model has no actual physical meaning for several related reasons.

(1) The accessible volume of the mobile phase is not constant but depends on the phenol concentration. Therefore, the stationary phase cannot be considered as identical from one adsorption data point to the next.
(2) The breakthrough curves corresponding to an S-shaped isotherm model should exhibit a diffuse front profile at low concentrations, not the front shock layer observed, see Fig. 2 (second column).
(3) The local isotherm curvature is not consistent with the elution profiles of large pulses of pure water (i.e. phenol vacancies) injected on the plateaus at 5 and 10 g/l (see Fig. 3). If the isotherm is locally convex downward (i.e. its tangent is below the curve as it is in the present case), the front part of the phenol vacancy should behave as the front of a large band of a compound with a Langmuirian isotherm and conversely [41,42], in contrast to what is ob-

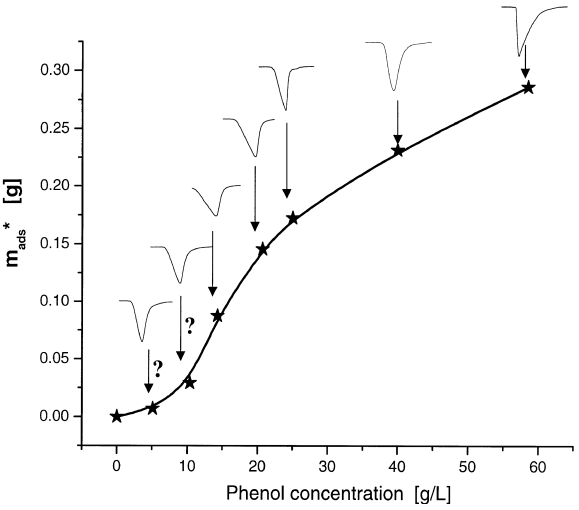

Fig. 3. Adsorption isotherm data (star symbols) of phenol on a C_{18}-Kromasil column, with pure water as the mobile phase. $T = 295$ K. Flow rate 1 ml/min. The chromatograms by each symbol are the elution profiles of a large pulse of pure water (i.e. a phenol vacancy). The question marks indicate that the band profiles are inconsistent with the curvature of the isotherm (see text).

served. At high concentrations, the apparent isotherm becomes convex upward, but the profiles of the large vacancies injected on the plateaus at 15, 20, 25, 40 and 60 g/l suggest a transition from a locally convex upward to a convex downward isotherm.

(4) The determination of convex downward isotherms by FA should be made by using negative breakthrough curves because these are those that give the shock layer that is consistent with the theoretical background of FA. This contradiction shows that the isotherm measured by FA does not correspond to the formation of a thermodynamic equilibrium.

The adsorption isotherm at a plateau concentration of 20 g/l was measured successively with two different initial conditions. For the first one, these conditions were as described earlier, leading to the results shown in Fig. 2 (fourth row). Just after the completion of this first run, however, the pump was not stopped, so the new initial state is one in which water occupies part of the mesopore volume. The hold-up volume measured in this case was about 2.5 versus 2.9 ml for the standard initial state (mesopores filled with water, Fig. 1). Then, the column was equilibrated with the same phenol solution as before the first run, at 20 g/l, for a second run. Fig. 4A compares the two breakthrough curves recorded. When water is present in the mesopores at the beginning of the FA run, the initial front is shifted toward longer retention times and is higher than the one observed with the standard initial state (no water in the mesopores). This can be explained by the fact that, when the mesopores are partly filled with water, the phenol molecules have faster and more complete access to the major part of the adsorbent surface so the retention of the front is stronger. If the mesopores are empty, by contrast, retention takes place only when the mobile phase wets the mesopore surface, a process which takes some time. At the end, however, the amount of phenol adsorbed at equilibrium is strictly the same (about 145 mg), suggesting that there is no distinction between the two final equilibrium states. The ways to reach it are simply different because the initial conditions are different and the mass transfer of the fluid into the pores that it wets is not instantaneous. We know from thin layer chromatography that the migration of the

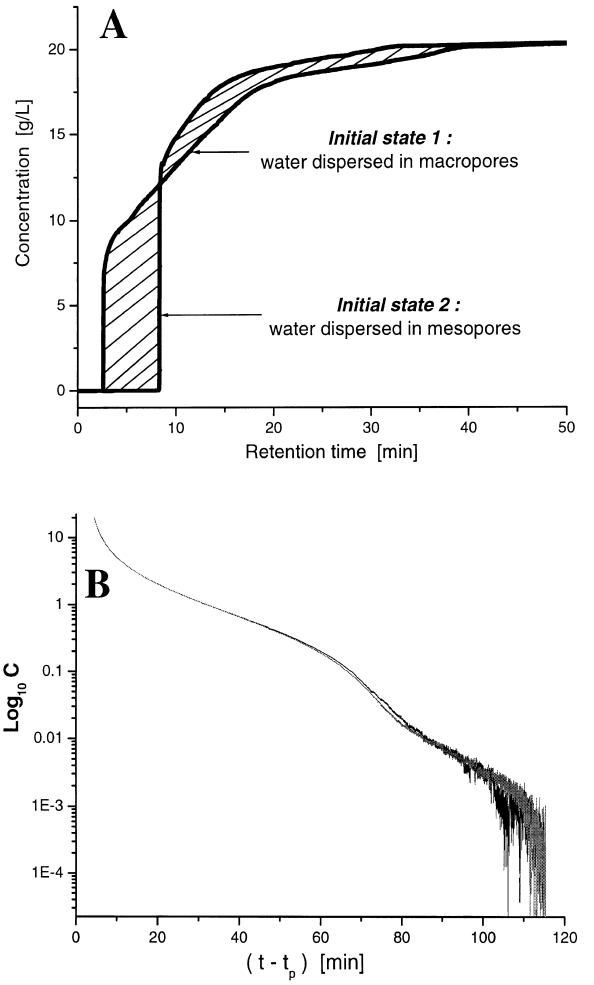

Fig. 4. Adsorption and desorption of phenol. (A) Influence of the initial state on the FA breakthrough curve of phenol for a constant plateau concentration of 20 g/l. C_{18}-Kromasil, pure water, $T = 295$ K. Flow rate 1 ml/min. Note the large difference between the two fronts. (B) Influence of the initial state on the desorption profile of phenol for a constant plateau concentration of 20 g/l. C_{18}-Kromasil, pure water, $T = 295$ K. Flow rate 1 ml/min. Note the similarity of the two curves.

fronts is slow, particularly when the contact angle is large [38].

To summarize, it is not possible to describe the adsorption behavior of phenol from the simple acquisition of FA measurements and the fitting of the corresponding data points. The profiles of the breakthrough curves calculated with the apparent adsorption isotherm obtained (Fig. 3) would have a disper-

sive part at low concentrations and a shock at high concentrations in contrast to experimental results. Actually, complex mass transfers and structure transformations take place between the mobile and the stationary phase and in the latter. They are probably controlled by the wetting rate of the C_{18}-bonded silica surface by the stream of new solution made to percolate through the column and to flush out the pure water. Although the adsorption profiles are difficult to handle properly, it is easy to derive the desorption isotherms from the desorption profiles recorded after the equilibration of the column has taken place. Fig. 4B compares the two desorption profiles recorded in the two experiments made with the same plateau concentration of 20 g/l, and the two different initial conditions. These two profiles are identical; they cannot be distinguished one from the other. The desorption is not influenced by the equilibration process used. The determination of the desorption isotherm using the FACP method is discussed later.

4.3. Desorption of phenol from the C_{18}-Kromasil column with pure water

The classical FACP method was applied to the six desorption profiles recorded following each of the FA experiments previously described. The major inconvenient of FACP is that these profiles depend on both thermodynamics and non-equilibrium effects. FACP would be exact only if the column were ideal, i.e. had an infinite efficiency. However, a real chromatographic column is never ideal. Hence, FACP suffers from a model error and the experimental isotherm derived from its data is only an approximation of the true isotherm. However, the efficiency of the column used (25×4.6 cm packed with 6 μm diameter spherical particles) is rather high, at around 15 000 plates under linear conditions, at a flow rate of 1 ml/min. Under such conditions, the model error is small and the isotherm derived by FACP is acceptable [18].

4.3.1. Adsorption–desorption hysteresis

The series of six desorption isotherms associated with the adsorption isotherms previously discussed is shown in Fig. 5 which exhibits six obvious hysteresis loops (the one at 40 g/l is not shown). Contrary to

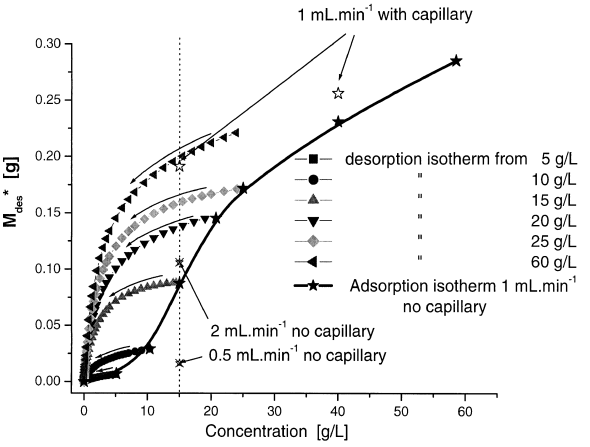

Fig. 5. Adsorption hysteresis. FA-adsorption and FACP-desorption isotherms of phenol on C_{18}-Kromasil with pure water as the mobile phase. $T = 295$ K. Flow rate 1 ml/min.

the adsorption process observed in FA, the desorption process of phenol observed in FACP is most probably thermodynamically controlled. During this process, the volume occupied by the mobile phase and the properties of the stationary phase remain ''frozen'' in a state that is imposed by the initial plateau concentration of phenol. This is the consequence of the metastable wetting of the C_{18}-silica surface by the water molecules that remain stable only as long as the pressure (hence, the flow rate) is kept constant in and along the column. Each desorption isotherm corresponds to the adsorption property of the stationary phase in a particular state (i.e. the mesopores of the particles being filled with a certain, constant amount of water). The desorption profiles (plotted in a logarithmic scale in Fig. 5) illustrate the difference of retention characteristics of the stationary phase depending on whether the desorption begins at a lower or higher phenol concentration in the mobile phase (see Fig. 2).

4.3.2. Estimation of the best physically consistent desorption isotherm

The set of six experimental desorption isotherms span most of the useful concentration range. These isotherms were determined using the FACP relationship between the retention time of a concentration and the isotherm. Using these isotherms to calculate these band profiles is obviously a circular argument,

all the more since no approximation and no model of adsorption have been assumed yet. Obviously, the agreement between experimental and calculated profiles (not shown) is excellent in the whole concentration range.

The determination of the best desorption isotherm raises three different problems. First, the selection of an appropriate isotherm model, second the determination of the best numerical coefficients of this model, and, third but not least, the interpretation of the results of this exercise. The desorption isotherms are obviously convex upward (Fig. 5). There are three simple possible models for such an isotherm, the Langmuir, the bi-Langmuir or the tri-Langmuir isotherms. The selection of these three models is reasonable since we have shown previously [36] that the isotherm of phenol in methanol/water solutions is properly modeled by the bi-Langmuir equation. Each of these three models was fitted to the six FACP isotherms, assuming three different weighing of the square residuals, $(q_{i,\mathrm{exp}}-q_{i,\mathrm{fit}})^2$, $1/q_{i,\mathrm{exp}}^2$, 1, and $q_{i,\mathrm{exp}}$. The relative importance of the high concentration data in the fit process increases in this order. The first weight assumes that constant relative errors are made in the measurement of the adsorption data and the second, constant absolute errors. The third weight gives considerable importance to the high concentration data which are deemed more significant in FACP because the model error [20] becomes important at low concentrations. The results of these different fits are reported in Table 2. The agreement between the fitting isotherm equation and the FACP isotherm data increases with increasing number of parameters in the isotherm model. The data fit always better to the tri-Langmuir isotherm than to the other two models.

In Fig. 6a–c, band profiles calculated with the three isotherm models (Langmuir, bi-Langmuir and tri-Langmuir) are compared with the corresponding experimental profiles. The comparisons are made successively for each one of the six initial equilibrium concentrations of phenol. As explained earlier, in each one of these six cases, there are three isotherms for each model, depending on the relative weight given to the experimental data. Only the best of these three calculated profiles is reported. Based on the large number of comparisons carried out (six different plateau concentrations and three weights for the isotherm fitting), it is reasonable to state that the bi-Langmuir model, despite a Fisher value that is lower than that of the tri-Langmuir model, accounts better for the elution profiles. For all the plateau concentrations involved, the bi-Langmuir model gives an excellent agreement between experimental and calculated profiles. Note that, for this isotherm model, only the weights 1 and $q_{i,\mathrm{exp}}$ give acceptable results, which suggests that the low concentration part of the desorption profile is controlled not only by the thermodynamics of adsorption equilibrium but also by the wetting of the stationary phase by the solution. This is also why the tri-Langmuir isotherm fails to describe the desorption profiles from the plateaus 15, 10 and 5 g/l.

The physical validity of the bi-Langmuir isotherm model is confirmed by the results of the calculation of the AED from the FACP isotherm data (Fig. 7). Since the initial part of the FACP isotherm is probably, to a significant extent, controlled by extra-thermodynamic effects, the low concentration data were truncated below 0.1 g/l. This concentration is smaller than 2% of the lowest plateau concentration used in the isotherm determinations. This threshold sets a maximum to the range of affinity constants that can be probed. Obvious bimodal distributions are obtained for all the concentration plateaus, except for the lowest one (5 g/l, not shown), which exhibits a divergence at low energies, due to the limited range of the concentrations that are sampled with a plateau at 5 g/l. There is a good agreement regarding the positions of the maxima of the adsorption energy of the two modes and the relative importance of their saturation capacities for the three highest concentration plateaus. Despite the truncation of the low concentration data, a non-zero saturation capacity is systematically obtained at the high end of the energy range. This means that the FACP isotherm obtained does not provide a linear relationship in the low concentration range and explains why the tri-Langmuir isotherm fits the adsorption data well.

When the concentration of phenol decreases from 60 to 20 g/l, the energies of the two modes of the AED remain constant while their saturation capacities decrease. This mirrors the decreasing amount of the mobile phase that penetrates into the mesopores. The concentration of 15 g/l corresponds to a threshold of the phenol concentration above which the

Table 2
Best isotherm parameters found for the fitting of the FACP adsorption data, according to the isotherm model (Langmuir, bi-Langmuir or tri-Langmuir) and the fitting weight chosen ($1/q_i^2$, 1 or q_i)

Equilibrium plateau concentration (g/l)	Isotherm model								
	Langmuir			bi-Langmuir			tri-Langmuir		
	$1/q_i^2$	1	q_i	$1/q_i^2$	1	q_i	$1/q_i^2$	1	q_i
							291.9	81.39	92.25
				3.906	4.525	**4.718**	0.024	0.133	0.1264
				0.287	0.210	**0.186**			
5	1.761	3.685	4.055				4.154	4.952	0.4836
	1.622	0.387	0.316				0.251	0.125	1.3630
				0.143	0.201	**0.256**			
				78.45	34.48	**16.11**	0.143	0.583	4.932
							41.85	1.115	0.1349
							13.09	12.50	12.47
				13.63	14.18	**13.44**	0.0588	0.0785	0.0740
				0.3963	0.1693	**0.1167**			
10	10.53	14.39	15.05				88.06	96.65	74.14
	0.8337	0.3824	0.3357				0.2402	0.2279	0.2467
				0.2829	3.061	**5.034**			
				74.21	1.950	**1.163**	7.841	7.001	7.239
							0.6624	0.7279	0.6998
							42.16	141.3	1254.5
				52.27	**52.13**	51.23	0.3678	0.3993	0.2199
				0.5282	**0.4505**	0.4356			
15	46.50	53.37	53.85			96.44	48.73	50.64	
	0.7909	0.5262	0.5059			0.4986	0.4141	0.4304	
				0.609	**2.381**	3.433			
				79.32	**7.398**	4.324	12.39	5.653	3.826
							1.1278	1.885	3.056
							1.1278	1.885	3.056
							61.22	56.48	52.31
				93.06	**65.54**	60.04	0.1059	0.0758	0.0574
				0.4516	**0.1129**	0.0873			
20	82.67	99.27	101.6				189.7	60.89	66.43
	0.658	0.3855	0.3516				0.5613	0.6612	0.5582
				0.7527	**48.39**	56.76			
				135.1	**0.8683**	0.7457	52.17	89.71	6.897
							0.7607	0.7625	2.583
							64.50	65.94	66.05
				127.8	90.46	**77.88**	0.1218	0.1265	0.1268
				0.4550	0.1847	**0.1516**			
25	114.5	133.3	135.3				79.54	77.83	77.71
	0.6952	0.4202	0.3898				0.7002	0.7124	0.7135
				1.602	52.25	**66.21**			
				84.19	1.076	**0.8763**	109.2	114.1	116.9
							1.2521	1.226	1.219
							109.4	107.2	139.3
				174.9	**108.2**	108.1	0.0359	0.0404	0.0104
				0.3764	**0.523**	0.04425			
60	161.3	183.4	187.1				127.4	124.9	80.1
	0.5411	0.3455	0.3156				0.5735	0.5862	0.2130
				2.737	**116.9**	123.6			
				18.41	**0.6519**	0.6104	45.6	45.5	0.8193
							0.9959	0.9517	79.59

Parameters are gathered by pairs. The first and second ones of each pair correspond to the saturation capacity ($q_{s,1}$, $q_{s,2}$ or $q_{s,3}$) and the associated adsorption constant (b_1, b_2 or b_3), respectively. The isotherm models, which best predict the desorption profiles are noticed in bold.

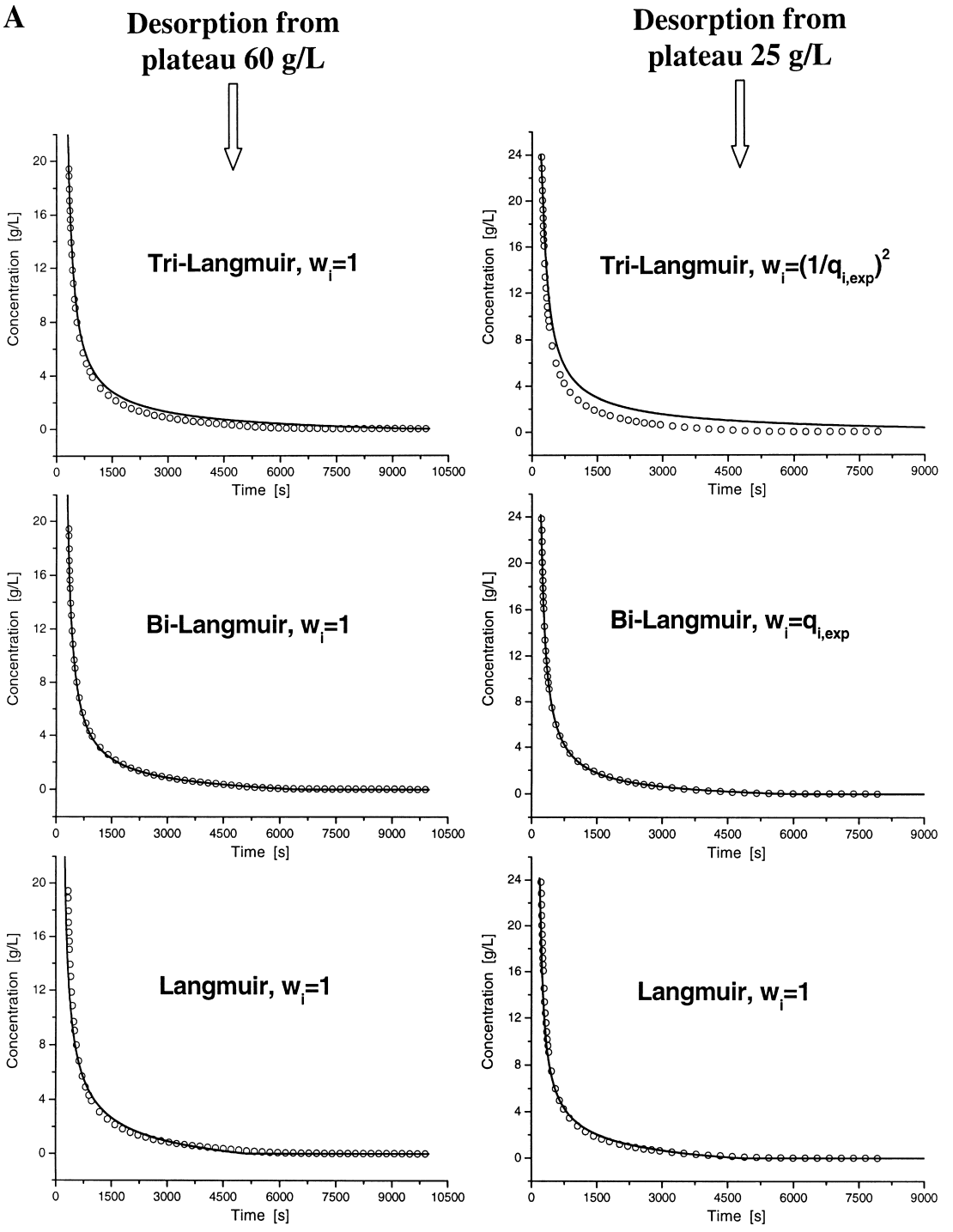

Fig. 6. Comparison between the six experimental desorption profiles and the profiles calculated with the ED model of chromatography and the desorption isotherms in Fig. 5.

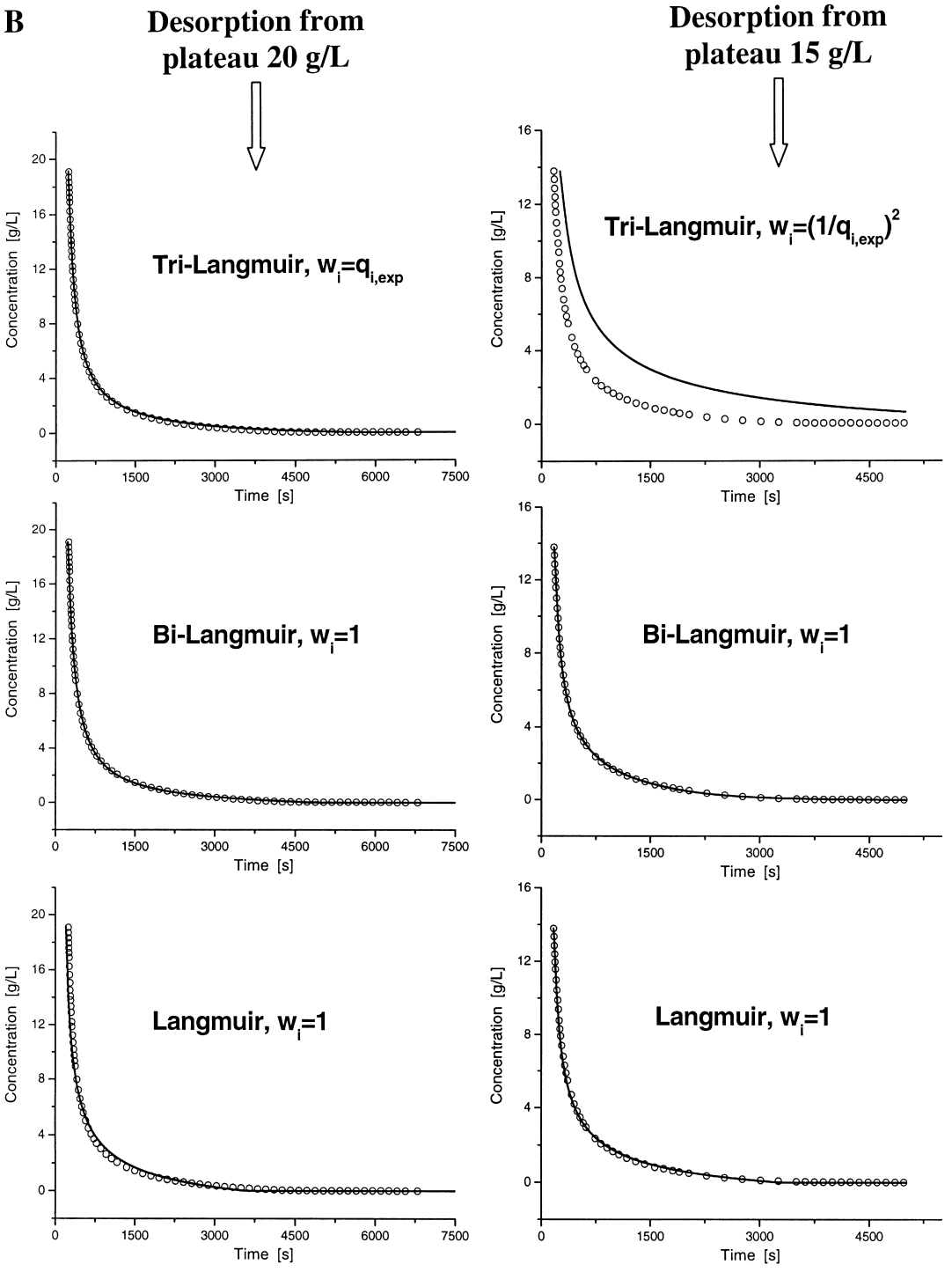

Fig. 6. (*continued*)

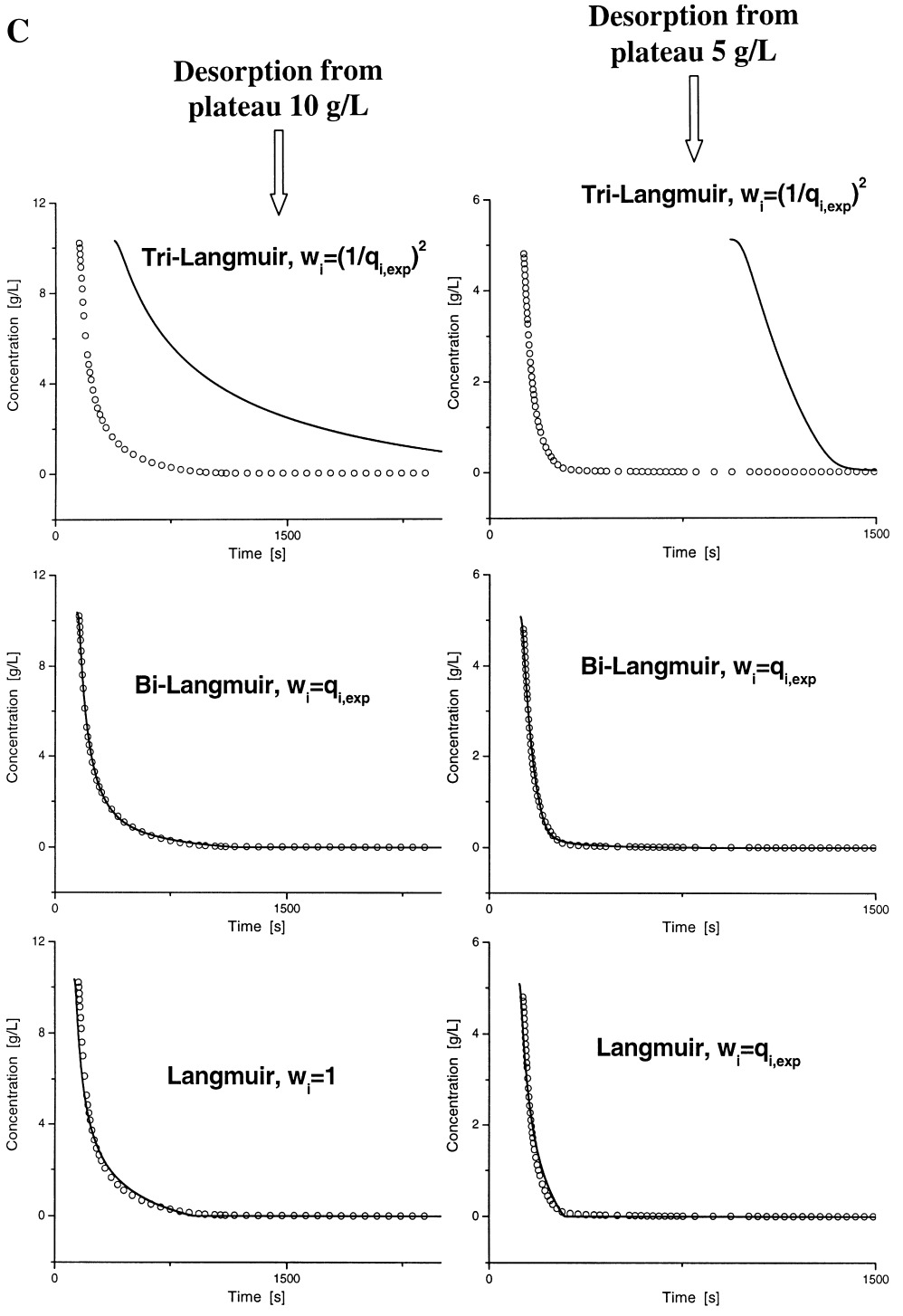

Fig. 6. (*continued*)

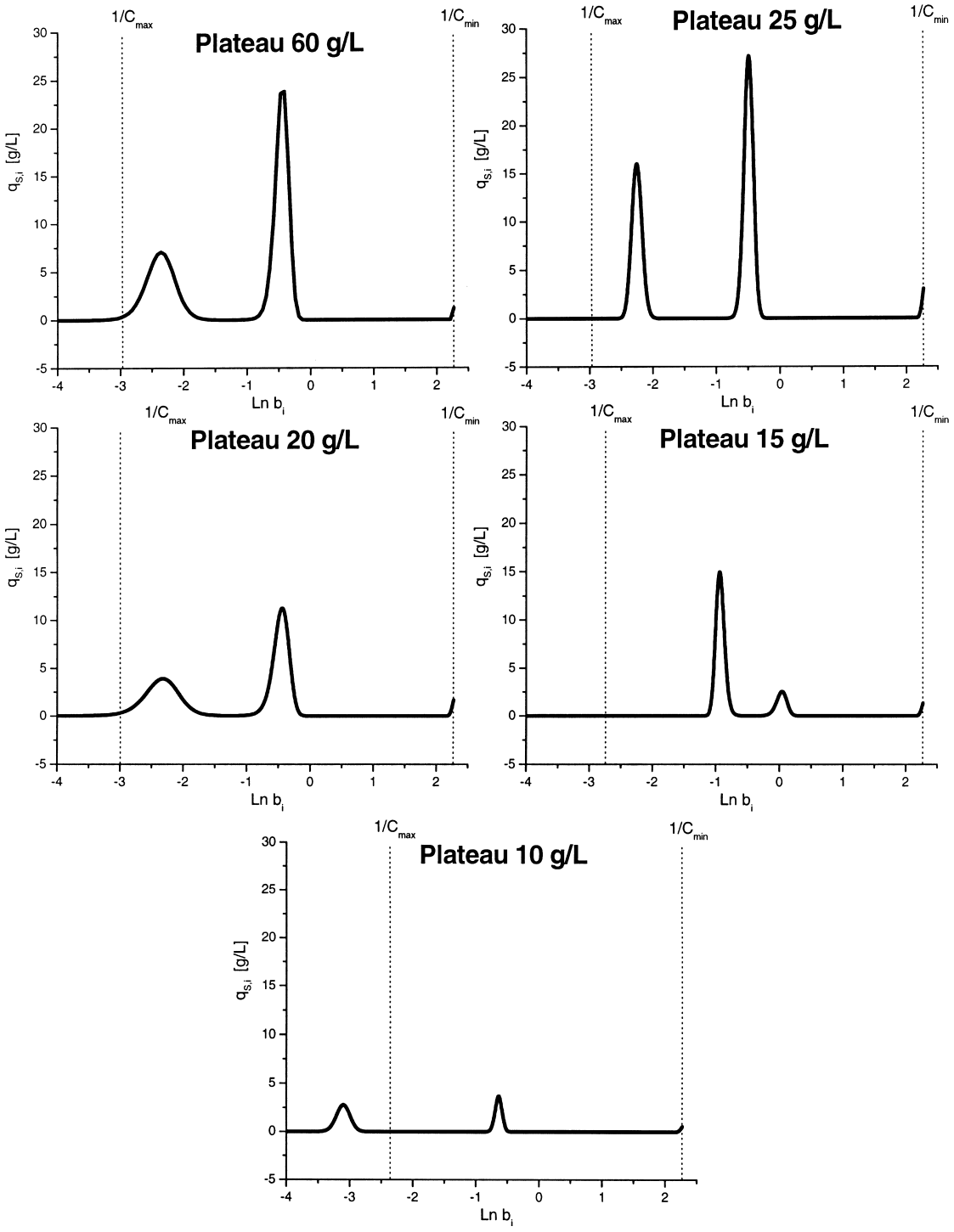

Fig. 7. AED (using 50 millions iterations) calculated from the experimental isotherm data measured by FACP and truncated at 0.1 g/l. Note the clear bimodal distribution found for the plateau concentrations of 60, 25, 20, 15 and 10 g/l. For 5 g/l, the calculation diverged at low energy due to the insufficient number of adsorption data points.

aqueous solution of phenol wets a significant proportion of the C_{18}-bonded silica surface and penetrates largely into the mesopore space (Fig. 8). Obviously, this threshold is a function of the pressure gradient along the column. Below this concentration, the two saturation capacities are small, showing that the mobile phase has little access to the mesopores. In a transition range, between 10 and 25 g/l, the two saturation capacities increase rapidly, tending toward values of the same order as those found for the saturation capacities in methanol/water solution. The adsorption energy decreases slowly with increasing phenol concentration, except for a local maximum at 15 g/l. Fig. 8 suggests also that the heterogeneity of the mesopore surface is higher at both ends of the concentration range ($C \leq 15$ and $C \geq 15$ g/l) than in the center.

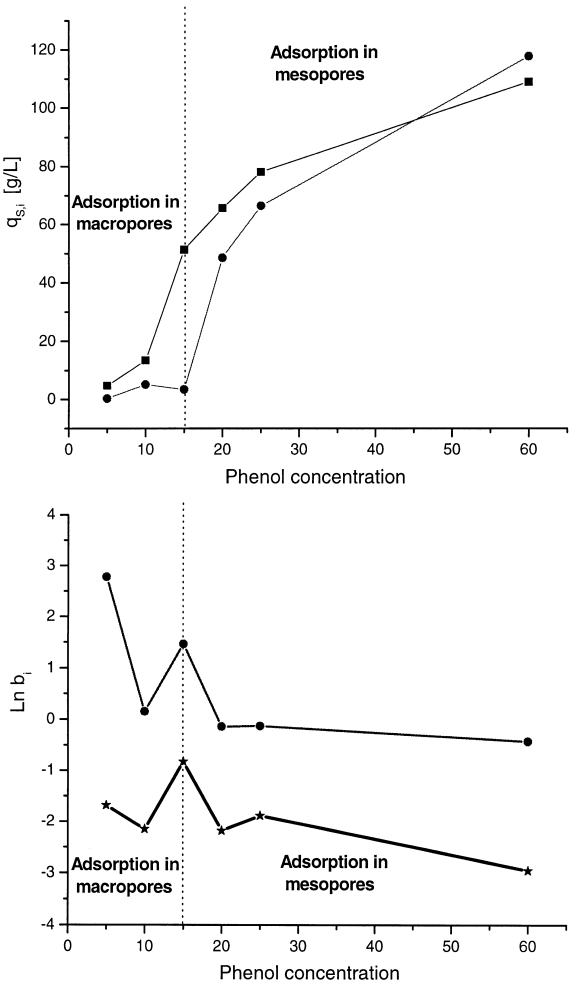

Fig. 8. Plots of the best parameters of the bi-Langmuir isotherms vs. the plateau concentration of phenol. Upper graph. Saturation capacities. Lower graph. Adsorption constant.

4.4. Influence of pressure on the apparent desorption isotherm

The Washburn equation shows that the average size of the pores that are filled under pressure by a fluid which has a contact angle larger than 90° on the surface is inversely proportional to the pressure applied [16]. Accordingly, the proportion of the pore volume of each particle filled by water or a water–phenol solution depends on its position along the column since the pressure decreases linearly from the column inlet to its outlet. Thus, the result obtained in the FA measurements should depend on the flow rate, since the local pressure everywhere in the column is approximately proportional to the flow rate (if the outlet pressure is neglected). The amount of phenol adsorbed in FA measurements should increase with increasing flow rate, which is what is observed (Fig. 5, star symbols). The amount adsorbed at 0.5 ml/min is extremely small, in agreement with the result of Washburn equation and with the pore size distribution of Kromasil that decreases dramatically above approximately 100 Å [16]. The fractional porosity flooded by water decreases rapidly with decreasing pressure, i.e. with decreasing flow rate.

This observation is also confirmed by the huge difference between the breakthrough curves recorded at different flow rates. Breakthrough curves recorded at 0.5, 1, and 2 ml/min are compared in Fig. 9. The difference between these curves is consistent with the Washburn equation and the pore size distribution of Kromasil [16]. Although this pore size distribution was measured with a lot different from the one used here, it was shown that the properties of this product are highly reproducible from lot-to-lot [35]. If a long thin capillary tube is connected downstream the detector, the pressions everywhere along the column are raised by the same amount. Fig. 9 shows also the breakthrough curve measured with a flow rate of 1 ml/min but pressures 140 bars higher than in the other cases. The profile of the breakthrough curves

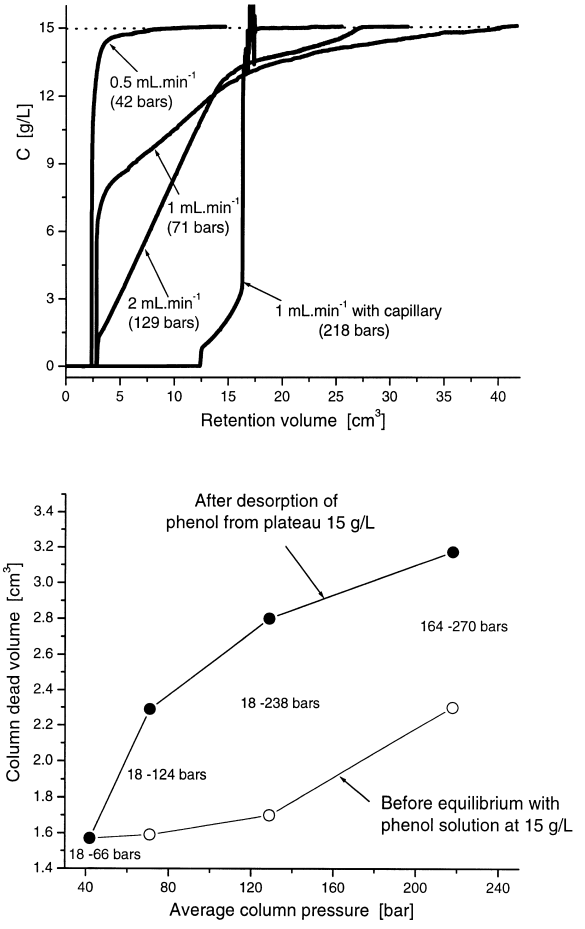

Fig. 9. Effect of the average column pressure and pressure gradient on the breakthrough curves of phenol in pure water. Plateau concentration: 15 g/l. Upper graph. Breakthrough curves. Lower graph. Plot of the hold-up volume vs. the average column pressure. The connecting tube between column and detector is narrow and causes an important pressure drop (18 bar at 1 ml/min).

becomes similar to the one recorded at 60 g/l, consistent with a much better wetting of the surface.

Finally, two data points obtained for breakthrough curves carried out with 15 and 60 g/l solutions with a capillary downstream the detector are reported in Fig. 5 (star symbols). It is significant that these two points, that both correspond to adsorption measurements, are on the highest desorption isotherm recorded (for 60 g/l). This suggest that under this high column pressure, the FA measurements are performed close to equilibrium conditions.

4.5. Determination of the parameters of the empirical adsorption isotherm in the case of a bi-Langmuir isotherm

As explained earlier, it is not possible to measure the adsorption isotherm of phenol in pure water by classical FA. The only parameters accessible to experimental determination are the desorption isotherms. The adsorption constant in pure water, derived from this isotherm under such conditions that the mobile phase has full access to the mesopore space, is compared in Fig. 10 to the values of this constant measured by FA when using aqueous solutions of methanol as the mobile phase [14]. The plot of the logarithm of the retention factor versus the fraction of MeOH in the mobile phase is linear and an LSSM seems to be valid in the range from 65 to 0% methanol. Fig. 10 also shows the plots of the logarithms of the contributions to the retention factor associated with each type of adsorption sites, calculated from the isotherm parameters and the column phase ratio ($F_{q_{s,i}} b_i$), and of the sum of these contributions versus the methanol content. There is an excellent agreement between the sum of the two contributions and the experimental value. Also, the plot of $\ln(F_{q_{s,1}} b_1)$ is nearly linear, suggesting that the

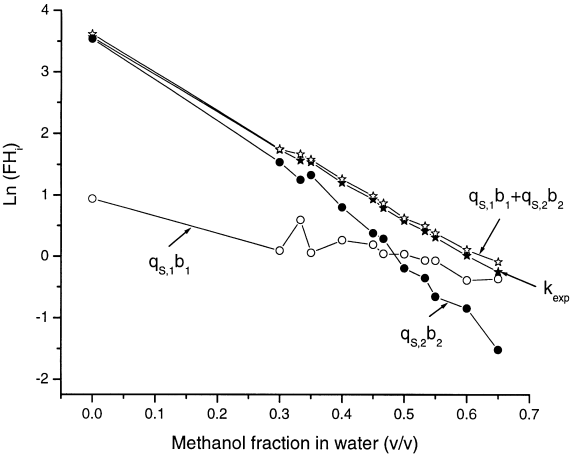

Fig. 10. Plots of the logarithm of the experimental and the calculated equilibrium constants of phenol on the C_{18}-Kromasil column and of the contributions of each type of sites i ($i=1$ low-energy sites; $i=2$ high-energy sites), $\ln(F_{q_{s,i}} b_i)$, to the retention, vs. the volume fraction of methanol in the mobile phase. k_{exp} is the experimental retention factor measured under linear conditions.

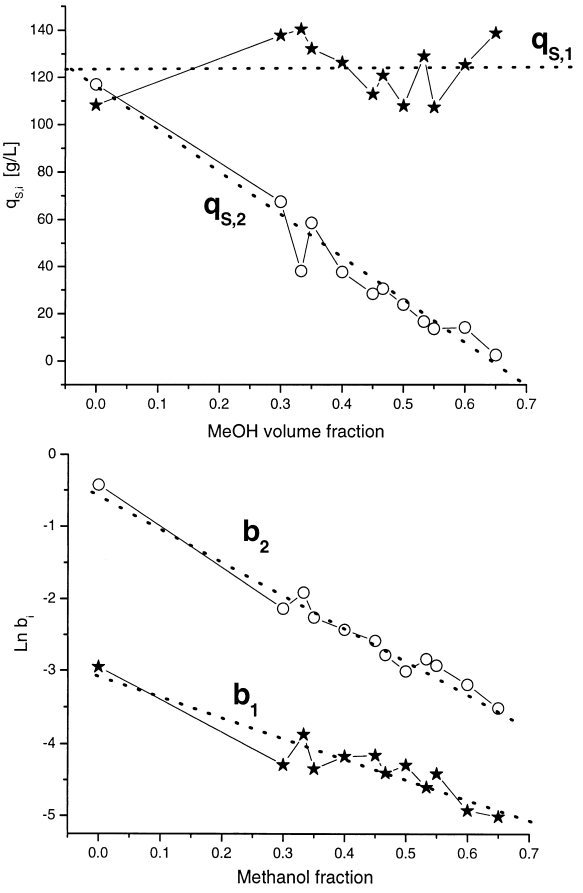

Fig. 11. Influence of the methanol concentration of the saturation capacity and the equilibrium constant of both types of sites. Upper graph. Plots of the saturation capacities of each type of sites ($i=1$ low-energy sites; $i=2$ high-energy sites) vs. the volume fraction of methanol in the mobile phase. Upper graph. Plots of the logarithm of the adsorption constant vs. the volume fraction of methanol in the mobile phase.

low energy sites follow the LSSM description. By contrast, this is not the case for the high energy sites. These results are explained in Fig. 11. The saturation capacity $q_{s,1}$ is nearly constant (ca. 125 g/l) while $q_{s,2}$ decreases linearly with increasing methanol content (Fig. 11, top). On the other hand, $\ln(b_1)$ and $\ln(b_2)$ decrease linearly with increasing methanol volume fraction in the mobile phase.

All these results suggest the following general empirical equation for the adsorption isotherm of phenol:

$$q^*(C,\varphi) = q_{1,0}\frac{b_{1,0}\exp(-S_{b_1}\varphi)C}{1+b_{1,0}\exp(-S_{b_1}\varphi)C} + (q_{2,0}-S_{q_2}\varphi)\frac{b_{2,0}\exp(-S_{b_2}\varphi)C}{1+b_{2,0}\exp(-S_{b_2}\varphi)C} \quad (20)$$

where the subcripts 1 and 2 refer to the low and high energy sites, respectively, $q_{1,0}$ is a constant, $b_{1,0}$ and S_{b_1} are the intercept and the slope of the plot of $\ln(b_1)$ versus the methanol fraction, φ, respectively, $q_{2,0}$ and S_{q_2} are the intercept and the slope of the plot of $q_{s,2}$ versus φ, respectively, and $b_{2,0}$ and S_{b_2} are the intercept and the slope of the slope of $\ln(b_2)$ versus φ, respectively. The best values of the parameters of this general isotherm are given in Table 3. Fig. 12 illustrates the agreement of this model with the experimental data. It compares the best estimates of the two contributions to the total retention under analytical conditions to the experimental ones for aqueous mobile phases containing between 0 and 65% methanol. These data provide the thermodynamic information required to calculate the band profiles of phenol under overloaded conditions, in isocratic or gradient elution chromatography.

5. Conclusion

Our results demonstrate that the adsorption of phenol from pure water onto a C_{18}-bonded silica surface is a complex phenomenon because pure water does not wet the surface but the phenol solution does, to an extent that depends on the phenol concentration in the mobile phase. Furthermore, the kinetics of the wetting is probably slow at

Table 3
Best empirical parameters coefficients of the general adsorption isotherm

$q_{1,0}$ (g/l)	$b_{1,0}$ (l/g)	S_{b_1}	$q_{2,0}$ (g/l)	S_{q_2} (g/l)	$b_{2,0}$ (l/g)	S_{b_2}
123.3	0.0464	2.840	111.3	171.7	0.5753	4.558

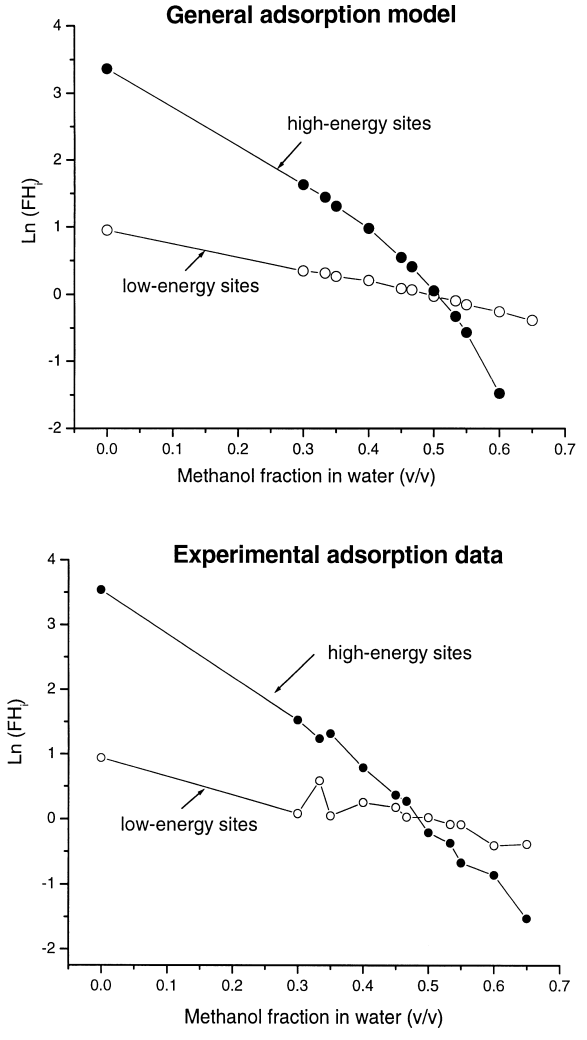

Fig. 12. General adsorption model of phenol on a RPLC column. Comparison between experimental and calculated adsorption isotherms. Upper graph. Combination of FA and FACP data in a general adsorption model (see text and Table 3). Lower graph. Plots of the logarithm of the contribution of each type of sites i ($i=1$ low-energy sites; $i=2$ high-energy sites) to the retention of phenol, $\ln(F_{q_{s,i}} b_i)$, on the C_{18}-Kromasil column under linear conditions vs. the volume fraction of methanol in the mobile phase.

the scale of liquid chromatography. So, because the kinetics of wetting is slow compared with the rate of migration of the breakthrough curve along the column, the stationary phase cannot be considered as the same adsorbent from one experiment to the next. The equilibrium properties of the chromatographic system (saturation capacities, adsorption constants) change to a large extent over the whole range of phenol solubility in pure water. By contrast, the kinetics of water repulsion is slow compared with the elution of the diffuse boundary of the breakthrough curve, so the surface remains constant during desorption. However, water expulsion takes place rapidly when the pressure is released from the column. One of the consequences of this phenomenon is a strong adsorption–desorption hysteresis when the initial state is a column whose mesopores are largely empty of water because the mobile phase stream was stopped. The adsorption curve follows an apparent S-shape isotherm model without physical meaning while the desorption curves are best modeled by a bi-Langmuir isotherm.

These results are consistent with previous results showing that the adsorption of phenol onto the same column from aqueous solutions of methanol with 30–65% methanol was accurately modeled by a bi-Langmuir isotherm. They allow the derivation of a general adsorption isotherm of phenol in RPLC. The validation of this isotherm will be discussed in a forthcoming paper by comparing the band profiles measured and calculated for large amounts of phenol eluted on the same C_{18}-Kromasil column under isocratic and gradient elution conditions.

Acknowledgements

This work was supported in part by grant CHE-00-70548 of the National Science Foundation and by the cooperative agreement between the University of Tennessee and the Oak Ridge National Laboratory. We thank Hans Liliedahl and Lars Torstenson (Eka Nobel) for the generous gift of the columns used in this work and for fruitful discussions.

References

[1] D.M. Ruthven, Principles of Adsorption and Adsorption Processes, Wiley, New York, NY, 1984.
[2] G. Guiochon, S.G. Shirazi, A.M. Katti, Fundamentals of Preparative and Nonlinear Chromatography, Academic Press, Boston, MA, 1994.
[3] D.M. Bliesner, K.B. Sentell, J. Chromatogr. 631 (1993) 23.
[4] D.M. Bliesner, K.B. Sentell, Anal. Chem. 65 (1993) 1819.

[5] J.L. Wysocki, K.B. Sentell, Anal. Chem. 70 (1998) 602.
[6] C.R. Yonker, T.A. Zwier, M.F. Burke, J. Chromatogr. 241 (1982) 257.
[7] C.R. Yonker, T.A. Zwier, M.F. Burke, J. Chromatogr. 241 (1982) 269.
[8] R.M. McCormick, B.L. Karger, Anal. Chem. 52 (1980) 2249.
[9] A. Berthod, I. Girard, C. Gonnet, Anal. Chem. 58 (1986) 1356.
[10] A. Berthod, I. Girard, C. Gonnet, Anal. Chem. 58 (1986) 1362.
[11] A. Berthod, A. Roussel, J. Chromatogr. 449 (1988) 349.
[12] M.F. Borderding, W.L. Hinze, Anal. Chem. 57 (1985) 2183.
[13] M.F. Borderding, W.L. Hinze, L.D. Stafford, G.W. Fulp, W.C. Hamlin, Anal. Chem. 61 (1989) 1353.
[14] F. Gritti, G. Guiochon, J. Chromatogr. A 995 (2003) 37.
[15] S. Golshan-Shirazi, G. Guiochon, Anal. Chem. (1989).
[16] H. Guan, G. Guiochon, E. Davis, K. Gulakowski, D.W. Smith, J. Chromatogr. A 773 (1997) 33.
[17] G. Guiochon, J. Chromatogr. A 965 (2002) 129.
[18] A. Felinger, G. Guiochon, J. Chromatogr. A 796 (1998) 59.
[19] G. Zhong, P. Sajonz, G. Guiochon, Ind. Eng. Chem. (Res.) 36 (1997) 506.
[20] H. Guan, B.J. Stanley, G. Guiochon, J. Chromatogr. A 659 (1994) 27.
[21] E. Glueckauf, Trans. Faraday Soc. 51 (1955) 1540.
[22] H. Poppe, J. Chromatogr. A 656 (1993) 19.
[23] Z. Ma, A. Katti, B. Lin, G. Guiochon, J. Phys. Chem. 94 (1990) 6911.
[24] M. Jaroniec, R. Madey, Physical Adsorption on Heterogeneous Solids, Elsevier, Amsterdam, 1988.
[25] D. Graham, J. Phys. Chem. 57 (1953) 665.
[26] R.J. Umpleby II, S.C. Baxter, Y. Chen, R.N. Shah, K.D. Shimizu, Anal. Chem. 73 (2001) 4584.
[27] J. Toth, Adsorption, Marcel Dekker, New York, NY, 2002.
[28] B.J. Stanley, S.E. Bialkowski, D.B. Marshall, Anal. Chem. 659 (1994) 27.
[29] M. Suzuki, Adsorption Engineering, Elsevier, Amsterdam, Netherlands, 1990.
[30] P.W. Danckwerts, Chem. Eng. Sci. 2 (1953) 1.
[31] K. Kaczmarski, M. Mazzotti, G. Storti, M. Morbidelli, Comput. Chem. Eng. 21 (1997) 641.
[32] K. Kaczmarski, Comput. Chem. Eng. 20 (1996) 49.
[33] K. Kaczmarski, D. Antos, J. Chromatogr. A 862 (1999) 1.
[34] P.N. Brown, A.C. Hindmarsh, G.D. Byrne, Procedure available from http://www.netlib.org.
[35] M. Kele, G. Guiochon, J. Chromatogr. A 855 (1999) 423.
[36] F. Gritti, G. Guiochon, J. Chromatogr. A 1003 (2003) 43.
[37] F. Riedo, M. Czencz, O. Liardon, E. sz Kovats, Helv. Chim. Acta 61 (1978) 1912.
[38] G. Guiochon, G. Körösi, A. Siouffi, J. Chromatogr. Sci. 18 (1980) 324.
[39] M. Al-Bokari, D. Cherrack, G. Guiochon, J. Chromatogr. A 975 (2002) 275.
[40] M. Diack, G. Guiochon, Langmuir 8 (1992) 1587.
[41] G. Zhong, T. Fornstedt, G. Guiochon, J. Chromatogr. A 734 (1996) 63.
[42] P. Sajonz, T. Yun, G. Zhong, T. Fornstedt, G. Guiochon, J. Chromatogr. A 734 (1996) 75.